HIGH POWER TEST RESULTS OF THE ELI-NP S-BAND GUN FABRICATED WITH THE NEW CLAMPING TECHNOLOGY WITHOUT BRAZING

D. Alesini, A. Battisti, M. Bellaveglia, A. Falone, A. Gallo, V. Lollo, D.T. Palmer, L. Pellegrino, L. Piersanti, S. Pioli, S. Tomassini, A. Variola, INFN-LNF, Frascati, Italy
L. Ficcadenti, V. Pettinacci, INFN Roma, Rome, Italy
F. Cardelli, L. Palumbo, University of Rome "La Sapienza", Rome, Italy

Abstract

High gradient RF photoguns have been a key development to enable several applications of high quality electron beams. They allow the generation of beams with very high peak current and low transverse emittance, thus satisfying the tight demands of free-electron lasers, energy recovery linacs, Compton/Thomson sources and high-energy linear colliders. A new fabrication technique for this type of structures has been recently developed and implemented at the Laboratories of Frascati of the National Institute of Nuclear Physics (INFN-LNF, Italy). It is based on the use of special RF-vacuum gaskets, that allow a brazing-free realization process. The S-band gun of the ELI-NP gamma beam system (GBS) has been fabricated with this new technique. It operates at 100 Hz with 120 MV/m cathode peak field and 1.5 μs long RF pulses to house the 32 bunches necessary to reach the target gamma flux. High gradient tests, performed at full power and full repetition rate, have shown extremely good performances of the structure in terms of breakdown rate. In the paper, we report and discuss all the experimental results, the electromagnetic design and the mechanical realization processes.

INTRODUCTION

Photocathode RF guns [1] allow reaching very high beam brightness and can find applications as injectors for FELs, TeraHertz and Compton sources and electron diffraction [2-15]. From the electromagnetic (e.m.) point of view, since the peak field at the cathode is proportional to the achievable beam brightness, in the last generation of RF guns a great effort has been put to increase the field amplitude, and, at the same time, to reduce breakdown rate probability (BDR) [16]. Standard RF guns fabrication is performed using brazing processes that require large vacuum furnaces, are very expensive and pose a not negligible risk of failure. Furthermore, BDR studies carried out on X-band prototypes indicated that, avoiding the high temperature thermal stress of copper associated with brazing, it is possible to reduce the BDR probability [15]. For all these reasons, a new brazing-free fabrication technique based on the use of special RF-vacuum gaskets has been recently developed at LNF-INFN [17] and successfully applied to the realization of a first RF gun prototype, currently in operation at UCLA at low rep. rate and relatively low cathode peak field [18].

This technique has been also adopted for the realization of the ELI-NP GBS [19] RF gun that has been tested at high power, reaching its nominal performances after 160 hours of operation. This test definitively demonstrates the reliability of this fabrication process for high gradient structures and its possible extension [20].

Table 1: Parameters of the ELI-NP RF gun (in parenthesis the measured values if different from the nominal ones).

Resonant frequency	2.856 [GHz]
$E_{cath}/\sqrt{P_{diss}}$	37.5 MV/(m·MW$^{0.5}$)
RF input power	14 MW
Cathode peak field	120 MV/m
Rep. rate	100 Hz
Quality factor	14600
Coupling coefficient	3 (2.5)
RF pulse length	1.5 μs
Rep. Rate (f_{rep})	100 Hz
Mode separation	41.3 MHz
E_{surf}/E_{cath}	0.9
Pulsed heating	<35 °C
Average diss. power	1.2 kW
Working temperature	30 deg.

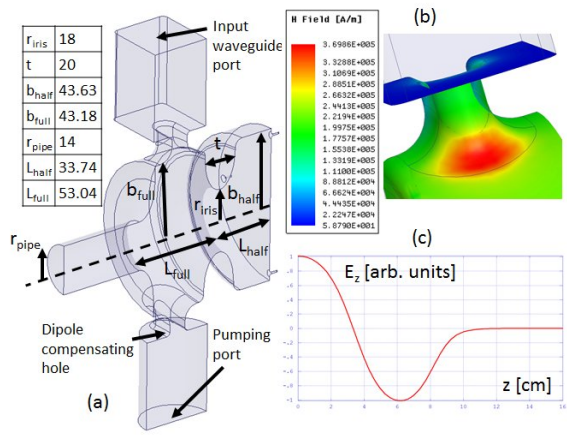

Figure 1: (a) HFSS geometry of the gun; (b) H field in the coupler region; (c) longitudinal accelerating field profile.

DESIGN CRITERIA

The design of the RF gun followed the same criteria illustrated in [18]. The main gun parameters are given in Table 1. The e.m. design of the gun has been done using 2D and 3D e.m. codes (Superfish [21] and Ansys [22]). Figure 1(a) shows the HFSS geometry of the gun with its main dimensions. In particular, the iris profile has been designed with an elliptical shape and a large aperture, to

ISBN 978-3-95450-182-3

simultaneously reduce the peak surface electric field, increase the frequency separation between the two resonant modes and improve the pumping efficiency on the half-cell. The coupling window between the rectangular waveguide and the full cell has been strongly rounded to reduce the peak surface magnetic field and, as a consequence, the pulsed heating [23]. Figures 1(b) and (c) show, respectively, the magnetic field in the coupler region at 120 MV/m cathode peak field and the longitudinal accelerating field profile. The coupling coefficient (β) has been chosen equal to 3 to allows both operation with short RF pulses and RF gymnastics to reach a uniform accelerating field over the 32 bunches train [19]. Furthermore, a high frequency separation of the resonant modes strongly reduces the residual field of the 0-mode due to the transient regime, which is particularly important if the structure is fed with short pulses [24]. Finally, to compensate the dipole field component, induced by the presence of the coupling hole, a symmetric port (connected to a circular pipe below cut off) has been included in the gun [25-27] and is also used as pumping port. The residual quadrupole field component due to the presence of the two holes does not affect the beam quality [28].

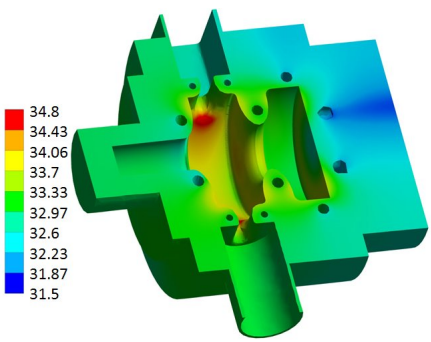

Figure 2: Gun temperature distribution under power.

The operation at 100 Hz with 1.5 μs RF pulses, required for the multi-bunch operation, results in an average dissipated power into the structure greater than 1 kW. A careful design of the cooling system has been done to avoid detuning of the gun during operation. The gun has 6 cooling channels with different diameters (Figs. 2 and 3): n.3 for the full cell, n.1 for the iris, n.1 for the half cell and n.1 for the cathode. The total water flow is 30 liter/min. The fully coupled thermal, structural and e.m. analysis, has been carried out in ANSYS Workbench [22], integrated by a specifically tailored APDL routine, following the same criteria illustrated in [29-31]. The calculated final temperature distribution is given in Fig. 2 and the corresponding deformations cause a detuning of the gun in operation lower than 100 kHz without affecting the field flatness. This detuning can be compensated changing the water inlet temperature of about 2 °C.

GUN FABRICATION

The mechanical drawings of the gun are shown in Fig. 3. The body of the gun has been fabricated from a single piece of OFHC copper using diamond tools. The rounded coupler geometry and the overall gun body have been realized with a 5 axis milling machine. The full cell has then been sealed clamping the body with the pipe by means of a special gasket, that simultaneously guarantees the vacuum seal and the RF contact avoiding sharp edges and gaps. The waveguide has been fabricated separately and its connection to the gun body have been obtained using a similar type of gasket.

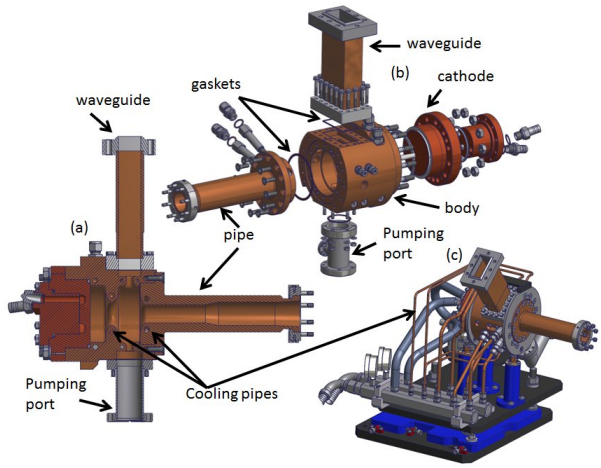

Figure 3: Gun mechanical drawings.

The device has been fabricated by a private company [32] with a precision on the internal dimensions of +/- 10 μm and roughness smaller than 150 nm. The detail of the gun assembly procedure is given in Fig. 3 (b). Also the cathode is fabricated from a single piece of copper and is clamped to the structure. The RF contact is guaranteed by pressure, while the vacuum seal by a special aluminium gasket not exposed to RF. Before the final clamping, the gun has been cleaned with a detergent (ALMECO-19), a mixture of organic (citric) acid and distilled water, in an ultra-sound bath. Pictures of the gun components before and after the clamping are given in Fig. 4.

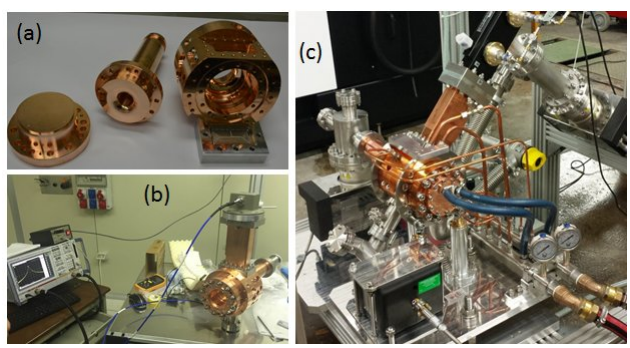

Figure 4: (a) gun components before clamping; (b) gun under low power test; (c) gun under high power test.

LOW AND HIGH POWER TEST

Low power RF test and tuning of the gun have been performed with the bead pull technique [33], measuring the reflection coefficient with a Network Analyzer. The picture of the structure under test is given in Fig. 4(b). The accelerating field profile and the reflection coefficient at the input port after tuning are given in Fig.

ISBN 978-3-95450-182-3

5. The tuning has been done by deformation tuners in the full cell. The resulting measured coupling coefficient was β=2.5 in fair agreement with the design value while all other parameters were in perfect agreement with the simulated ones.

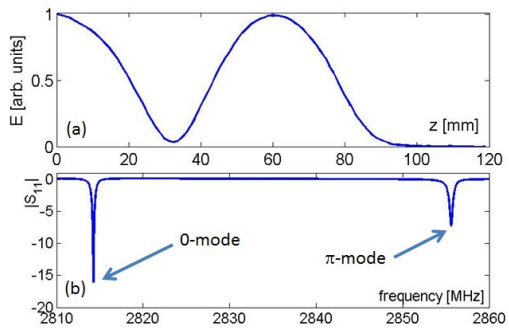

Figure 5: (a) measured E field; (b) measured refl. coeff.

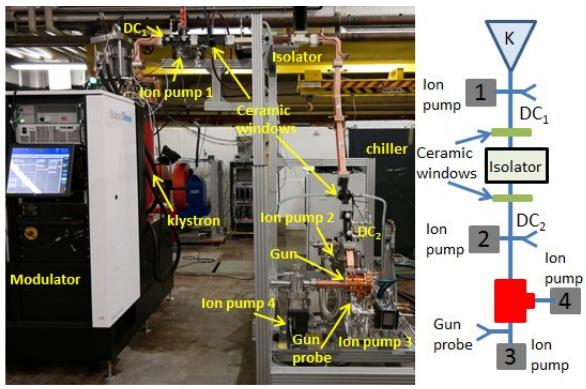

Figure 6: High power setup and schematic layout.

High power RF tests have been performed at the Bonn University under RI responsibility [34]. Pictures of the structure and test stand are given in Fig. 4(c) and 6. The power source was the ELI-NP Scandinova RF Unit based on Solid State modulator K2-3 and 60MW S-band Toshiba klystron. Two directional couplers (DC) have been inserted in the waveguide line to detect the forward and reflected power signals right after the klystron and before the gun. Four ion pumps have been connected following the same configuration of the final ELI-NP injector. An isolator in SF6 has been also inserted to protect the klystron from the reflected power.

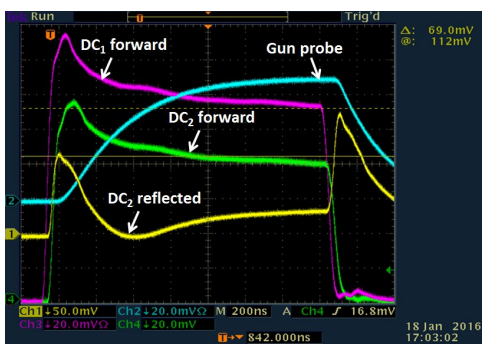

Figure 7: RF signals measured during high power test.

The aim of the test was to achieve 120 MV/m at the cathode (corresponding to 14 MW input power) at the nominal repetition rate of 100 Hz with 1.5 μs RF pulse duration. The power signals from DCs were measured using diodes and oscilloscopes. Samples of the detected signals are given in Fig. 7. The klystron power, rep. rate and pulse length were progressively increased and breakdown phenomena were detected looking at the ion pumps current absorption and RF signals from pickups. Figure 8 shows the conditioning history. The conditioning procedure was semi-automatic and the power has been increased acting on modulator High Voltage (HV). In particular, the switch-off of the modulator HV could be caused by: (a) ion pumps current absorption exceeding a threshold corresponding to a pressure of 5×10^{-8} mbar; (b) high reflected power to the klystron; (c) distortions of the reflected signal due to breakdown phenomena. This last control method has been implemented using a fast PXI system and is thoroughly illustrated in [35]. The waveform at each pulse was compared with the previous one within a mask of tolerance and, in case of pulse distortions due to a discharge, the modulator was switched off immediately. This method allows a very fast and sensitive control of the breakdown events with respect to the control based on vacuum pressure only. The RF conditioning lasted about 160 hours and the gun finally reached the nominal parameters with a break down rate of few 10^{-5} bpp. The vacuum pressure was measured by the ion pumps current during the whole process. It was of the order of 1×10^{-8} mbar at full power and always maintained a decreasing trend. At the end of conditioning and without power the vacuum pressure in the gun was lower than 5×10^{-10} mbar.

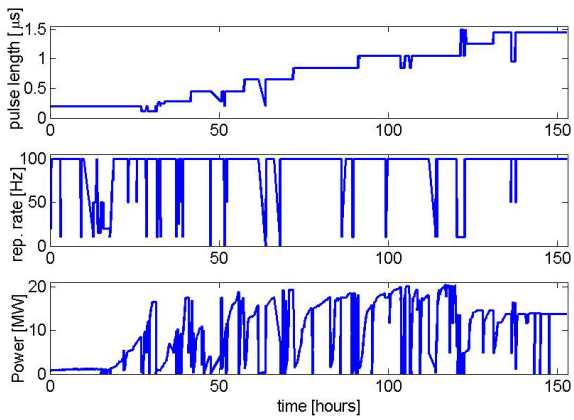

Figure 8: RF pulse length, input power and rep. rate as a function of time during the high power test.

CONCLUSIONS

The S-band gun of the ELI-NP GBS has been fabricated with a new technique recently developed and implemented at the INFN-LNF and based on the use of special RF-vacuum gaskets that allow a brazing-free assembling processes. The structure has been successfully tested at high power and it reached in a remarkable short time (160 hours) the nominal parameters (120 MV/m cathode peak field at 100 Hz and 1.5 μs RF pulse length). The tests definitively demonstrate the reliability and suitability of such fabrication process for high gradient structures realization.

REFERENCES

[1] D.Palmer PhD thesis "The next Generation Photoinjector", June 1998.

[2] P.G. O'Shea *et al.*, in *Proc. PAC'91*, 1991, p. 2754.

[3] D.H. Dowell *et al.*, *Appl. Phys. Lett.* 63 (1993) 2035.

[4] R. Dei-Cas *et al.*, Nucl. Instr. and Meth. A 296 (1990) 209.

[5] S. Schreiber, in Proc. EPAC2000, 2000, p. 309.

[6] R. Akre *et al.*, *Phys. Rev. ST Accel. Beams* 11 (2008) 030703.

[7] H.S. Kang and S.H. Nam, in *Proc. FEL'10*, 2010, p. 155.

[8] R. Kuroda, *Nucl. Instr. and Meth. A* 593 (2008) 91.

[9] C. Yim *et al.*, in *Proc. IPAC'10*, 2010, p. 1059.

[10] J.B. Hasting *et al.*, *Appl. Phys. Lett.* 89 (2006) 184109.

[11] R. Li *et al.*, *Rev. Sci. Instrum.* 80 (2009) 083303.

[12] J. Yang *et al.*, *Rad. Phys. Chem.* 78 (2009) 1106.

[13] P. Musumeci *et al.*, *Rev. Sci. Instrum.* 82 (2010) 013306.

[14] J.-H. Han, *Phys. Rev. ST Accel. Beams* 14 (2011) 050101.

[15] R. Kuroda *et al.*, *Nucl. Instr. and Meth.* A 637 (2011) S183.

[16] V.A. Dolgashev *et al.*, "RF breakdown in normal conducting single-cell structures", in *Proc. PAC05*, May 2005, Knoxville, Tennessee, U.S.A.

[17] Int'l patent application PCT/IB2016/051464, D. Alesini *et al.*, "Process for manufacturing a vacuum and radio-frequency metal gasket and structure incorporating it" assigned to INFN.

[18] David Alesini *et al.*, "New technology based on clamping for high gradient radio frequency photogun", PRST- AB 18, 092001 (2015).

[19] O. Adriani *et al.*, Technical design report EuroGammaS proposal for the ELI-NP gamma beam system scientific Editor L. Serafini, arXiv:1407.3669

[20] F. Cardelli *et al.*, in *Proc. IPAC2016*, Busan, Korea, 2016, p. 403.

[21] http://laacg.lanl.gov/laacg/services/download_sf.phtml

[22] http://www.ansys.com

[23] V. A. Dolgashev *et al.*, "RF breakdown in normal conducting single-cell structures", in *Proc. PAC'05*, Knoxville, TN, 2005 (IEEE, Piscataway, NJ, 2005).

[24] C. Limborg *et al.*, "RF Design of the LCLS Gun", LCLS-TN-05-3, www-ssrl.slac.stanford.edu/lcls/technotes/LCLS-TN-05-3.pdf

[25] D. T. Palmer, R. H. Miller and H. Winick, "Microwave Measurements of the BNL/SLAC/UCLA 1.6 Cell Photocathode RF Gun", in *Proc. PAC'95*, USA, 1995, p. 982.

[26] X. Guan, C. Tang, H. Ghen, W. Huang, X. He, P. Xu and R. Li, *Nucl. Instrum. Methods Phys. Res.*, Sect. A 574, 17, 2007.

[27] M. S. Chae *et al.*, "Emittance growth due to multipole transverse magnetic modes in an rf gun", PRST-AB 14, 104203, 2011.

[28] A. Bacci and A. Giribono, private communications.

[29] V. Pettinacci *et al.*, in *Proc. IPAC'14*, Dresden, Germany, 2014, p. 3860.

[30] D. Alesini, L. Pellegrino, V. Pettinacci *et al.*, "Thermal Analysis of a Radiofrequency Gun", ("Innovabook 2014" - Paper Anthology, Fluidodinamica, Meccanica, Elettromagnetismo - Cobalto Casa Editrice).

[31] D. Alesini *et al.*, Design of high gradient, high repetition rate damped C-band rf structures, PR AB 20, 032004 , 2017.

[32] http://www.comeb.it

[33] J. Maier *et al.*, "Field measurements in resonant cavities," *Journal of applied physics*, vol. 23, no. 1, pp. 68–77, 1952.

[34] http://research-instruments.de/

[35] S. Pioli *et al.*, "The Real-Time Waveform Mask Interlock System for the RF Gun Conditioning of the ELI-NP Gamma Beam System", presented at IPAC'17, Copenhagen, Denmark, May 2017, papper TUPIK057, this conference.

ISBN 978-3-95450-182-3